ORIGINAL PAPER

Sustainable utilization of incinerated paper mill sludge ash for the manufacture of building bricks

Balaji Govindan[1] · Vidhya Kumarasamy[2]

Abstract

Fly ash–lime–gypsum bricks are an environmentally friendly and energy-efficient alternative to burnt clay bricks. Nowadays, the scarcity of fly ash and lime adversely affects the production of fly ash bricks. To mitigate this, the current study examines incinerated paper mill sludge ash as a supplement to fly ash and lime. In the current study, in blend 1, coal fly ash is replaced by incinerated paper mill sludge ash (2.5–30 wt%), and in blend 2, lime is completely replaced by incinerated paper mill sludge ash (2.5–15 wt%). Based on Indian standards, bricks were tested for compressive strength, water absorption, weight density, percentage voids, efflorescence, drying shrinkage, dynamic modulus of elasticity, and impact energy. Before developing bricks, the materials have to be examined by X-ray diffraction, X-ray fluorescence, Fourier transform infrared spectroscopy, thermogravimetry differential thermal analysis, and scanning electron microscope techniques. Results from X-ray diffraction showed that higher replacement of incinerated paper mill sludge ash does not produce any phase transformation and merely improves porosity, which reduces weight. Higher replacement of incinerated paper mill sludge ash leads to a reduction in strength and a higher water requirement. The study found that incorporating incinerated paper mill sludge ash at replacement 2.5–15 wt% in blend 1 and 2.5–5 wt% in blend 2 satisfied the building brick requirements. By incorporating incinerated paper mill sludge ash into bricks, the brick industry can produce sustainable bricks that utilize resources effectively.

Graphical Abstract

Graphical abstract illustrating the reuse of incinerated paper mill sludge ash in the manufacturing of building bricks to minimize the demand for fly ash and lime. The visual shows the drawbacks of paper mill sludge in land dumping, the suggested methodology for reusing incinerated paper mill sludge ash to minimize environmental degradation, improved sustainability through waste utilization, its benefits, and the characterization of bricks.

✉ Balaji Govindan
balaji.anbu465@gmail.com; balajig.civil@mkce.ac.in

Vidhya Kumarasamy
vidhya22047@gmail.com

1 Department of Civil Engineering, M.Kumarasamy College of Engineering, Karur, Tamilnadu, India

2 Department of Civil Engineering, Mahendra Engineering College, Namakkal, Tamilnadu, India
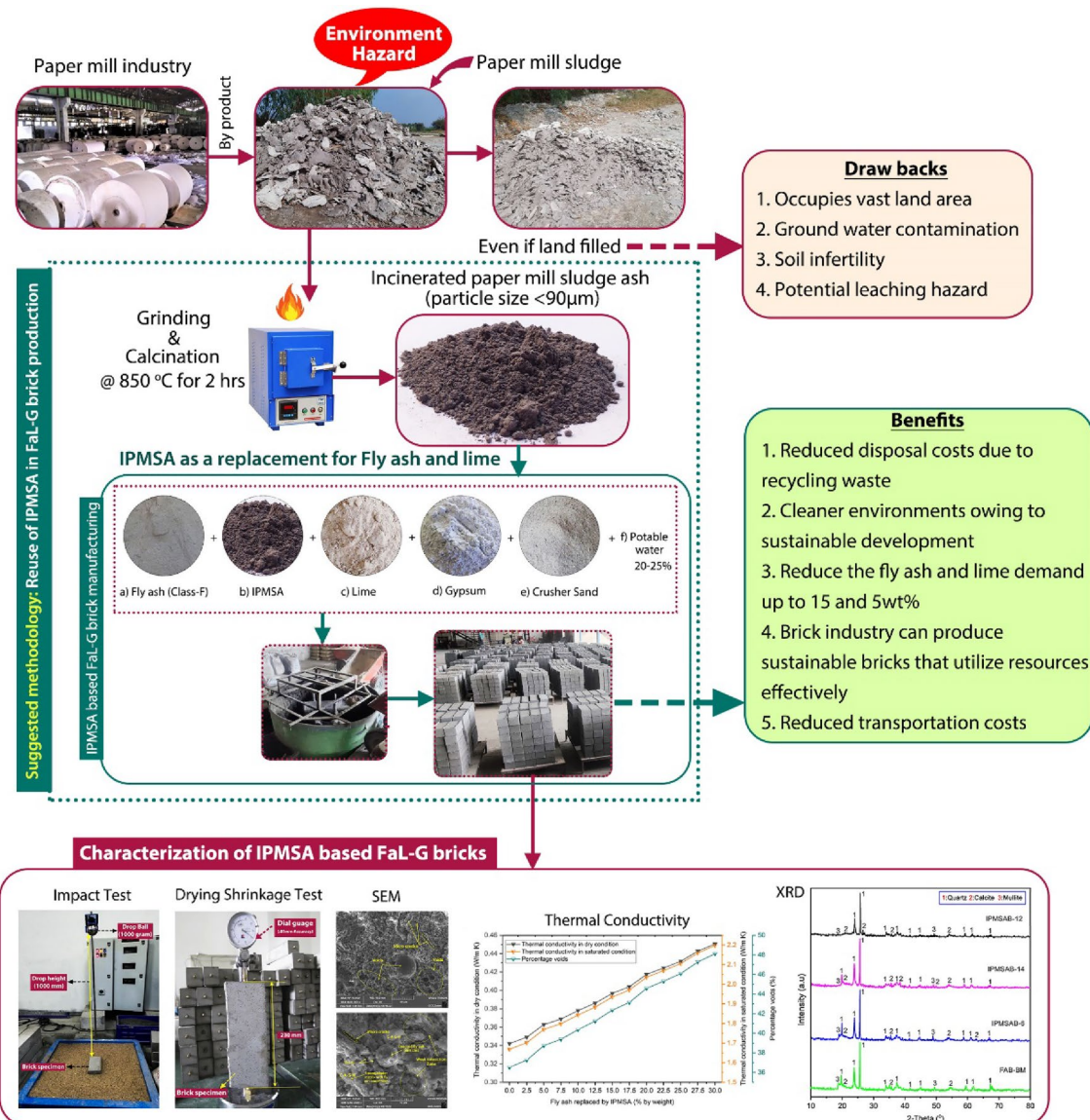
Introduction

Masonry bricks have been an essential building material in the construction industry for a long time. Aside from its high strength, low production costs, and durability, it has played a significant role in construction (Chin et al. 2022). Before concrete and other recent construction materials became prevalent in the Asian region, clay bricks were widely used. In recent decades, Brick construction was a popular choice due to its ease of manufacturing using surface soil and low construction cost. During the making of fired brick, the brick kilns emit several gases, including CO_2, SO_2, and others,

which also deplete enormous amounts of land. There is a growing concern about the environment arising from these emissions and consumptions in many countries (Cicek and Tanrıverdi 2007). In order to develop sustainable building practices, it is essential to produce unfired bricks.

Fly ash has been used as an industrial by-product to reduce clay's negative environmental impact in brick production as a replacement for clay. Thermal power plants produce fly ash as a by-product of burning pulverized coal. ASTM (ASTM C618:2012) divides fly ash into two categories: Class F and Class C. Construction industries are encouraged to use bulk fly ash as a safe way to dispose of polluting fly ash. It is important to note, however, that cementitious binders are detrimental to the environment because of their associated carbon dioxide emissions. It is therefore undoubtedly the most efficient way to reduce

carbon footprints through the use of cementitious binders and pozzolana, particularly fly ash. But, in India for the past two years the demand for alternative supplementary cementitious materials (SCMs) is essential as the widely used SCMs such as fly ash are in limited supply and have a major impact on fly ash–lime–gypsum (FaL-G brick) production, i.e., the rate at which fly ash is exploited varies greatly among Indian states. There is a range of 35 to 98% in different states due to ash stocks can be cleared in states with a high utilization rate. A large accumulation of ash stocks can cause pollution in states with low utilization rates. The ash in such areas accumulates in slurry form together with water in ash ponds, and it accumulates in dry form across public lands. Due to this shortage, fly ash supplies are lower than expected, and its duration is unknown. The cement sector is its primary user, but it has not gained

much from its massive growth over the years, despite its huge use so far. There has been an increase of nearly 78% in cement production in India between 2009 and 2019. In response to growing demand, this number is projected to rise to 400 million tonnes by 2025. For the past years, it has had a significant impact on the production of FaL-G bricks (CSE analysis 2021).

Unfired brick technology also uses alkaline activated agents as a binder and industrial by-products as a renewable resource to produce aggregate binder (Sutcu et al. 2014). Activators such as lime are made from crushed limestone that has been calcined for a certain period of time at 1000–1200 °C to remove carbon dioxide molecules, and then it is ground into powder. The overmining and consumption of crushed limestone, a non-renewable natural resource, will cause significant environmental harm, including the eradication of vegetation, soil erosion, loss of water, encroachment on open space, and pollution of the environment. In order to create a more environmentally friendly society and industry, waste materials will be used in place of lime.

To overcome the above stated problems, alternative building materials are being developed to reduce environmental impact and meet criteria for sustained development, manufacturing, and consumption because improving sustainability is one of the most challenging tasks facing the construction industry (Balaguera et al. 2018). It aids in preserving the environment and reducing the cost of disposal in landfills. In civil engineering, various studies have investigated the use of recycled and other waste materials as alternatives in brick production. Recycled blast furnace slag, industrial lime waste, incinerated sewage ash, stone dust, rice husk ash, cement kiln dust are a few examples (Gencel et al. 2012).

Another renewable waste material known as "incinerated paper mill sludge ash (IPMSA)", which is produced by paper mills, is a by-product of the incineration of pulp and paper mill sludge. As of 2015 (Indian paper industry: out of the woods 2016), India produced roughly 13 million tonnes of paper, paper board, and newsprint each year, which is 3.18% of the world's total production. As a result, solid waste accumulates and is dumped in landfills, raising environmental issues. In the past, it has been attempted to use paper mill sludge for various applications, including cementitious products, fiberboards, polymer reinforcement, and hydraulic binders, as it contains belite, metakaolinite, tricalcium aluminate, belite, gehlenite, and mayenite (Frías et al. 2015). In spite of this, the presence of CaO and MgO in sludge makes it unsuitable for a full replacement, so it is only used as a partial replacement for cementitious binders up to 10%. The incorporation rate of paper mill ashes in cement-based composites may be limited due to swelling issues due to high levels of free lime (Zmamou et al. 2021). The higher absorption of water by paper sludge in cement mortar or concrete reduces the flow properties. In recent studies, paper sludge has been used in

anaerobic digestion, gasification, steam reforming, direct liquefaction, and pyrolysis methods for energy recovery (Deviatkin et al. 2015). IPMSA can be used as a resource material in the manufacture of bricks and will have several advantages, including: 1) reduced disposal costs due to recycling waste, 2) cleaner environments owing to sustainable development, and 3) reduced transportation costs (Raut et al. 2012). Still the IPMSA is replaced by fly ash and lime in FaL-G bricks is not, however, used. The relationship between apparent porosity and thermal conductivity for Fal-G building bricks incorporated with IPMSA was not attempted to be established.

In the construction sector, there is an increasing demand for energy-efficient structures. IPMSA is an ideal solution to meet this demand for reusing and recycling waste. This will solve both the waste management problem and serve as a supplementary resource for the construction industry. By using IPMSA in the production of unfired bricks, this paper addresses sustainability from three points of view (environmental, social, and economic). The IPMSA supplements were adjusted in accordance with Bureau of Indian Standards (BIS) recommendations (IS 1077:1992; IS 3495 (Parts 1 to 4):1992; IS 12894:2002). The utilization of these bricks on an industrial application promotes in sustainable and economic development.

The present study provided a new method to reuse IPMSA in FaL-G brick production to supplement fly ash and lime. The excessive addition of IPMSA will generally result in a significant reduction in the strength of hardened bricks. Using the IPMSA as a supplement in FaL-G bricks with the optimum mix proportion makes this work novel because it satisfies the building brick requirement as per BIS (IS 12894:2002). Incorporating IPMSA into these unfired bricks facilitates the reutilization of paper mill sludge in large-scale construction projects.

Materials and methods

Materials

Fly ash of class F confirming to BIS (IS 3812 (Part-1):2003) used for this study was collected from a thermal power station in Mettur, Tamil Nadu, India. Paper mill sludge is a by-product of the deinking and re-pulping of paper. It is collected from Tamil Nadu Newsprint and Paper Limited (TNPL), Kagithapuram, Karur. Brick manufacturing does not directly use the raw paper mill sludge. The raw paper mill sludge is processed by grinding it to a consistent weight, and then drying it at 105 °C. Next, it undergoes calcination in a muffle furnace for 2 h at a temperature of 850 °C. This results in an ignition loss of 35.85% at 850 °C, transforming the material into ash (Furlani et al. 2008). The resulting IPMSA is then cooled to room temperature and grounded

again (particle size < 90 μm). Hydrated lime of "Class C" as per BIS (IS 712:1984). It is obtained from Karur, Tamil Nadu, India. Gypsum is procured from Kanish Plaster, Coimbatore, Tamil Nadu. Crusher sand is procured from Sri Ganesh Murugan Blue Metals, Karur, Tamil Nadu. For the entire experimental investigation, potable water is used for production, curing, and other testing purposes as per BIS (IS 456:2000). Table 1 depicts the physical properties of the materials used in this investigation.

Mix proportion and casting methodology of FaL-G bricks incorporated with IPMSA

Fly ash, IPMSA, lime, crusher sand, gypsum, and potable water are the primary material used to cast the bricks in present study. In the entire investigation, two different blends were used. In blend 1, 12 mix combinations are tested to find the optimum mix where fly ash is replaced by IPMSA up to 30 wt%. According to the previous studies, lime, crusher sand, and gypsum are fixed at 15, 20, and 5 wt%, respectively (Sivasakthivadivelan. 2022). FAB-BM represents the FaL-G brick without using IPMSA (base mix). In blend 2 (6 mix combinations) where the lime is completely replaced by IPMSA up to 15 wt%. Here, fly ash, crusher sand and gypsum are fixed at 60, 20 and 5 wt%, respectively. Table 2 shows the mix combinations of IPMSA based FaL-G bricks.

As per Table 2, fly ash, IPMSA, crusher sand, lime, and gypsum in proper proportions are thoroughly mixed in a dry pan mixer, and then water is added until a homogeneous mixture is formed. To obtain plastic conditions for binary mixes, the optimal quantity of water (ie., 0.10 × wt. of (fly ash + lime + crusher sand + gypsum) + 0.15 × wt. of IPMSA) was maintained in mix. Despite IPMSA high water demand, the quantity of water was kept more. In order to control the mixes under wet conditions, water was added in a measured quantity (by weight of the dry mix). The materials had to be mixed lump-free for about 30 min. Furthermore, the wet mix was checked for uniformity of moisture distribution by using the oven drying method specified by BIS (IS 2720 (part II): 1973). The mixture is then transported to automatic brick making hydraulic die machine by a belt conveyor, where a pressure of 40 tons is applied to form "FaL-G bricks incorporated with IPMSA". Then the casted bricks

are transferred to wooden pallets and sun dried in the open air for 48 h, thereafter, transported to open area where it is water cured for 28 days. The actual size of the brick cast in the entire investigation is 230 × 105 × 75 mm. Figure 1 shows the experimental methodology including process of IPMSA making, characterization of materials and bricks, and manufacturing process of the FaL-G bricks incorporated with IPMSA.

Testing methods

Casted brick specimens were tested for compressive strength using a 1000 kN universal testing machine (UTM), water absorption, and efflorescence of the samples was determined as per BIS (IS 3495 (Parts 1 to 4):1992). In order to determine the density, the mass of the FaL-G brick specimens was divided by its volume at room temperature. As per ASTM (ASTM C642:2021), the percentage voids were calculated.

Brick impact energy (I_e) was determined using a drop test on full-size bricks measuring 230 mm × 105 mm × 75 mm as shown in Fig. 2a. The brick samples were subjected to a 1000 g steel ball being dropped from a fixed free height of 1000 mm. This study used a modified test setup to determine the impact resistance of hardened bricks similar to previous studies (Saxena et al. 2018) using concrete specimens. It was noted number of blows were required for the development of the first visible crack (N_i) and the specimens final failure (N_f). The impact energy of FaL-G brick specimen has been obtained using the following equation (Eq. 1) (Saxena et al. 2018).

$$I_e = N_i mgh \tag{1}$$

where N_i = No. of drops for the first visible crack, m = Mass of the steel drop ball, g = Gravity (9.81 m/s²), h = Drop height in mm

Full-size bricks were put through a non-destructive test to determine the ultrasonic pulse velocity (UPV) of hardened bricks in accordance with BIS (IS 13311 (Part 1):1992). On 28-day-cured samples, the observed UPV has been used to compute the dynamic modulus of elasticity (E_d). In recent studies on related cementitious materials (Gupta et al. 2016), the dynamic modulus of elasticity was calculated using the equation (Eq. 2) presented below.

$$E_d = \frac{\rho V^2}{g} * 10^{-2} \tag{2}$$

where E_d = Dynamic modulus of elasticity in GPa, ρ = Weight Density in kg/m³, g = Acceleration due to gravity (9.81 m/s²), V^2 = Ultrasonic pulse velocity in km/s

Drying shrinkage have been conducted for the test specimens as per the guidelines of BIS (IS 4139:1989). Figure 2b

Table 1 Physical properties of materials

Physical properties	Lime	fly ash	IPMSA	Crusher sand
Specific gravity	2.26	2.30	1.72	3.20
Surface area in m²/kg	1235	992	4230	1286
Bulk density in kg/m³	1520	1140	1260	1750
Lime reactivity in kg/cm²	–	2.62	1.87	–

Table 2 Mix combinations (blends 1 and 2)

S. no	Mix ID	Blend	Materials used for brick production in % by weight				
			Fly ash	IPMSA	Lime	Crusher Sand	Gypsum
1	FAB-BM	Blend 1 (fly ash replaced by IPMSA)	60	0	15	20	5
2	IPMSAB-1		57.5	2.5	15	20	5
3	IPMSAB-2		55	5	15	20	5
4	IPMSAB-3		52.5	7.5	15	20	5
5	IPMSAB-4		50	10	15	20	5
6	IPMSAB-5		47.5	12.5	15	20	5
7	IPMSAB-6		45	15	15	20	5
8	IPMSAB-7		42.5	17.5	15	20	5
9	IPMSAB-8		40	20	15	20	5
10	IPMSAB-9		37.5	22.5	15	20	5
11	IPMSAB-10		35	25	15	20	5
12	IPMSAB-11		32.5	27.5	15	20	5
13	IPMSAB-12		30	30	15	20	5
14	IPMSAB-13	Blend 2 (lime replaced by IPMSA)	60	2.5	12.5	20	5
15	IPMSAB-14		60	5	10	20	5
16	IPMSAB-15		60	7.5	7.5	20	5
17	IPMSAB-16		60	10	5	20	5
18	IPMSAB-17		60	12.5	2.5	20	5
19	IPMSAB-18		60	15	0	20	5

depicts the drying shrinkage test setup. With the help of a dial gauge and a drying shrinkage apparatus, bricks wet and dry lengths were measured. The thermal conductivity of FaL-G bricks was tested using a quick thermal conductivity meter (QTM-500, Kyoto Electronics, New Castle). Under completely dry, and saturated conditions and at room temperature, QTM-500 was used to test the thermal conductivity of materials.

Chemical and mineralogical characterization

To determine their chemical and mineral compositions, raw materials underwent X-ray fluorescence (XRF) and X-ray diffraction (XRD) analyses. The analysis was performed on a Bruker S4 Pioneer spectrometer for XRF and an Empyrean, Malvern Panalytical X-ray diffractometer with Co source Cu $K\alpha$ ($\lambda = 1.54$ Å) for XRD. A laser scattering diffraction particle size distribution analyzer (Partica LA-950) was used to measure the particle size distributions with a range of particle sizes between 10 and 3 mm. A dry powdered sample was scanned using Fourier transform infrared (FT-IR) spectroscopy (PerkinElmer) using KBr pellets made from powdered samples to obtain the compound structure of IPMSA. The microstructure of FaL-G brick specimens and raw material samples were examined using a scanning electron microscope (SEM) SEM VEGA3 TESCAN. The brick specimens were examined at 500 and 2000× with SEM, while the photographs were taken at 2000× with an accelerated voltage of 15 kV with SEM.

Results and discussion

Characterization of raw materials

Gradation of materials

Figure 3a–d shows the particle size distribution of fly ash, IPMSA, crusher sand, and lime. It was found that fly ash, lime, IPMSA, and crusher sand all had a wide variety of particle sizes. Fly ash particle size ranges from 0 to 100 µm, with an average diameter (D_{50}) of 20 to 30 µm. It has been shown by many studies (Lind and Grahn 2011) that fly ash particles exhibit a bimodal distribution. The lime used in this study has particles that are between 10 and 105 µm in size. Similarly, the particle size of the IPMSA varies from 1 to 1000 µm. As a result, although the IPMSA has a larger specific surface area than the other materials, it is significantly finer. According to BIS (IS 383:2016), crusher sand is classified as zone II and is used as a fine aggregate.

Chemical composition

Table 3 shows the chemical composition of fly ash. IPMSA, and lime. More than 70% of fly ash is composed of silicon dioxide (SiO_2), aluminum oxide (Al_2O_3), and calcium oxide (CaO), which are its predominant compositions. Titanium dioxide (TiO_2), Potassium Oxide (K_2O), Phosphorus pentoxide (P_2O_5), Sodium Oxide (Na_2O), Sulfur trioxide (SO_3),

Fig. 1 Experimental methodology
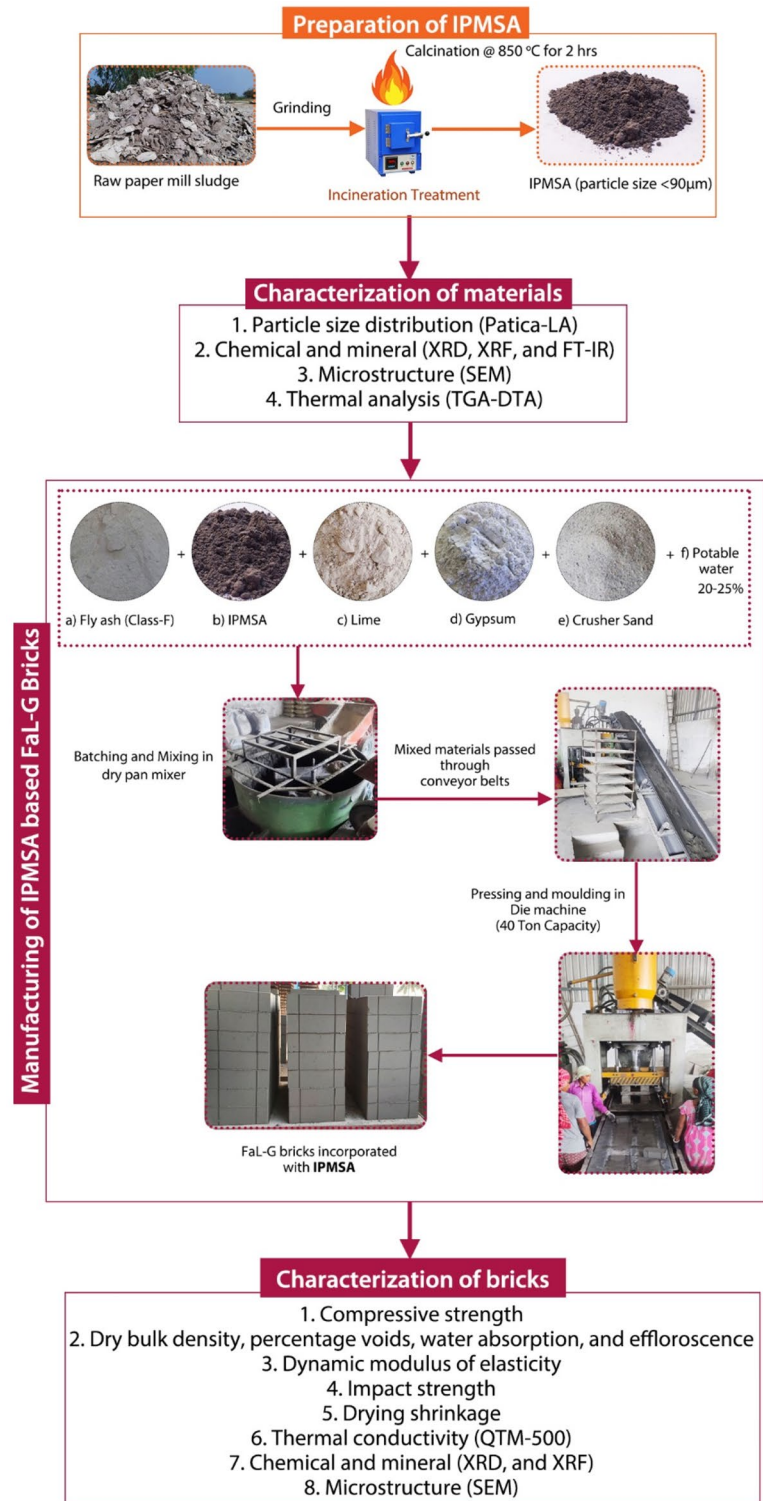
Iron Oxide (Fe$_2$O$_3$), and Magnesium Oxide (MgO) can be detected at a trace level, less than 5 wt%. Because it contains more silica, alumina, and iron oxide (more than 70%), and less calcium oxide, this fly ash is classified as Class F according to IS 3812 (part 1):2003 (IS 3812 (Part-1):2003). IPMSA is primarily composed of lime (CaO), alumina

(Al$_2$O$_3$) and silica (SiO$_2$). There is a high loss of ignition (LOI) associated with the high concentration of carbonates and organic compounds (Goel and Kalamdhad 2017). The major oxide present in the lime was (CaO). Extremely low concentrations of MgO, Fe$_2$O$_3$, Al$_2$O$_3$ and SiO$_2$ are present in lime.
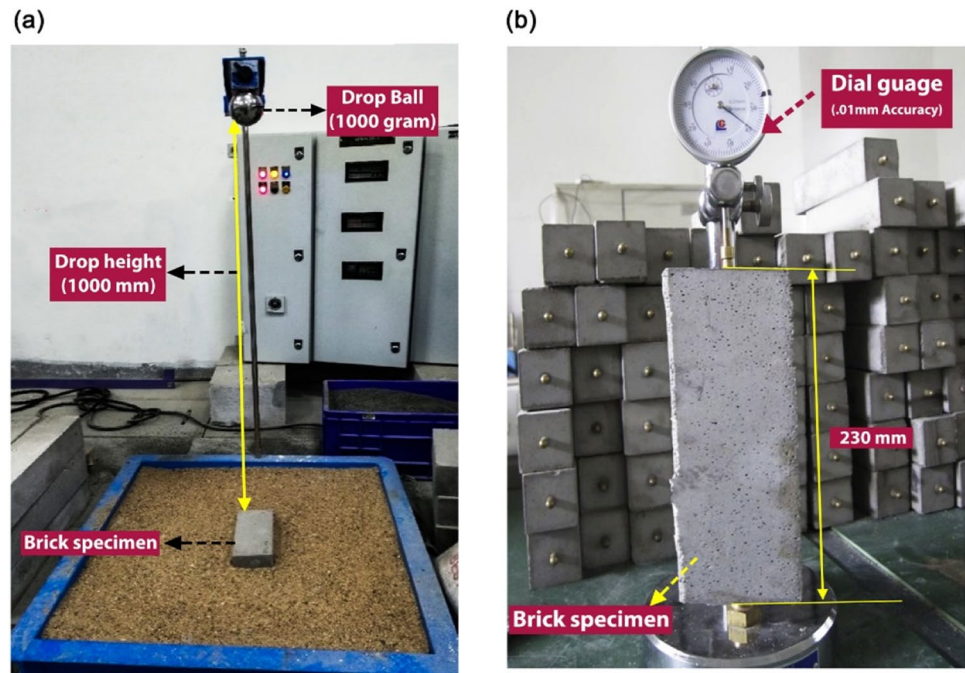
Figure 4a shows the XRD pattern of fly ash, IPMSA and lime. As can be seen from the hump in the slag curve, several amorphous substances are present, and it is possible to distinguish several crystals that are carbonates. Quartz (SiO_2), mullite ($3Al_2O_3 \cdot 2SiO_2$), magnesium calcite ($Mg_{0.03}Ca_{0.97}(CO_3)$), calcite ($CaCO_3$), anhydrite ($CaSO_4$), lime (CaO), portlandite ($Ca(OH)_2$), and mullite ((($3Al_2O_3 \cdot 2SiO_2$) crystals are found in fly ash. In contrast to the weak peaks of SiO_2, corundum (Al_2O_3), and kaolinite ($Al_2O_3\ 2SiO_2 \cdot 2H_2O$), the IPMSA pattern reveals the presence of high calcite peaks. IPMSA contains primarily $CaCO_3$, which is a form of calcium. Similar XRD patterns for IPMSA have been seen in earlier studies (Goel and Kalamdhad 2017). Similarly, the lime XRD pattern contains high CaO peaks, while $Ca(OH)_2$ and $CaCO_3$ have weak peaks.

Compound structure of IPMSA can be determined by FT-IR spectroscopy. It has been confirmed that IPMSA contains lignocellulose in nature. A characteristic peak of the OH group ($3395\ cm^{-1}$) can be found in Fig. 4b, along with a C–H stretch for saturated aliphatic molecules ($2869\ cm^{-1}$) and a C–H bending ($1363\ cm^{-1}$), aromatic stretching (1760 cm-1), C–O stretching ($10{,}870\ cm^{-1}$), and C–C stretching ($936\ cm^{-1}$) contains lignin, cellulose, and hemicellulose (Coates 2006). Along with hydrocarbons, there is the presence of carbonates (2484 and $796\ cm^{-1}$).

Surface morphology

The surface morphologies of fly ash, IPMSA, and lime are shown in Fig. 5a–i, respectively. The physical view of fly ash, IPMSA, and lime is depicted in Fig. 5a and d, and g, respectively. The SEM micrographs of 500 and 2000× magnifications of fly ash are shown in Fig. 5b–c, respectively. It is found that the fly ash particles are smooth spheres in shape. Pores are observed on the surface of relatively large particles. However, its properties are similar to those of cement. The SEM micrographs of 500 and 2000× magnifications of the IPMSA are shown in Fig. 5e–f, respectively. There is a heterogeneous mixture of particle sizes and shapes in IPMSA. In the SEM images, thin crystalline layers are seen on inorganic particles with an angular and asymmetrical shape. Due to their hydrophilic nature, these amorphous particles are able to draw water into their pores during hydration of the oxides (Grau et al. 2015). There are several agglomerated particles as well as a few spherical ones. The SEM micrographs of 500 and 2000× magnifications of lime are shown in Fig. 5h–i, respectively. Compared to the other materials, the SEM micrographs of lime are agglomerated and formed into a larger crystal structure, but the overall crystal size was smaller than the fly ash and larger than the IPMSA.

Characterization of IPMSA based FaL-G building bricks

Compressive strength

The most important critical index for FaL-G bricks is compressive strength. The relationship between the average compressive strength of IPMSA-based FaL-G bricks and percentage decrease in compressive strength
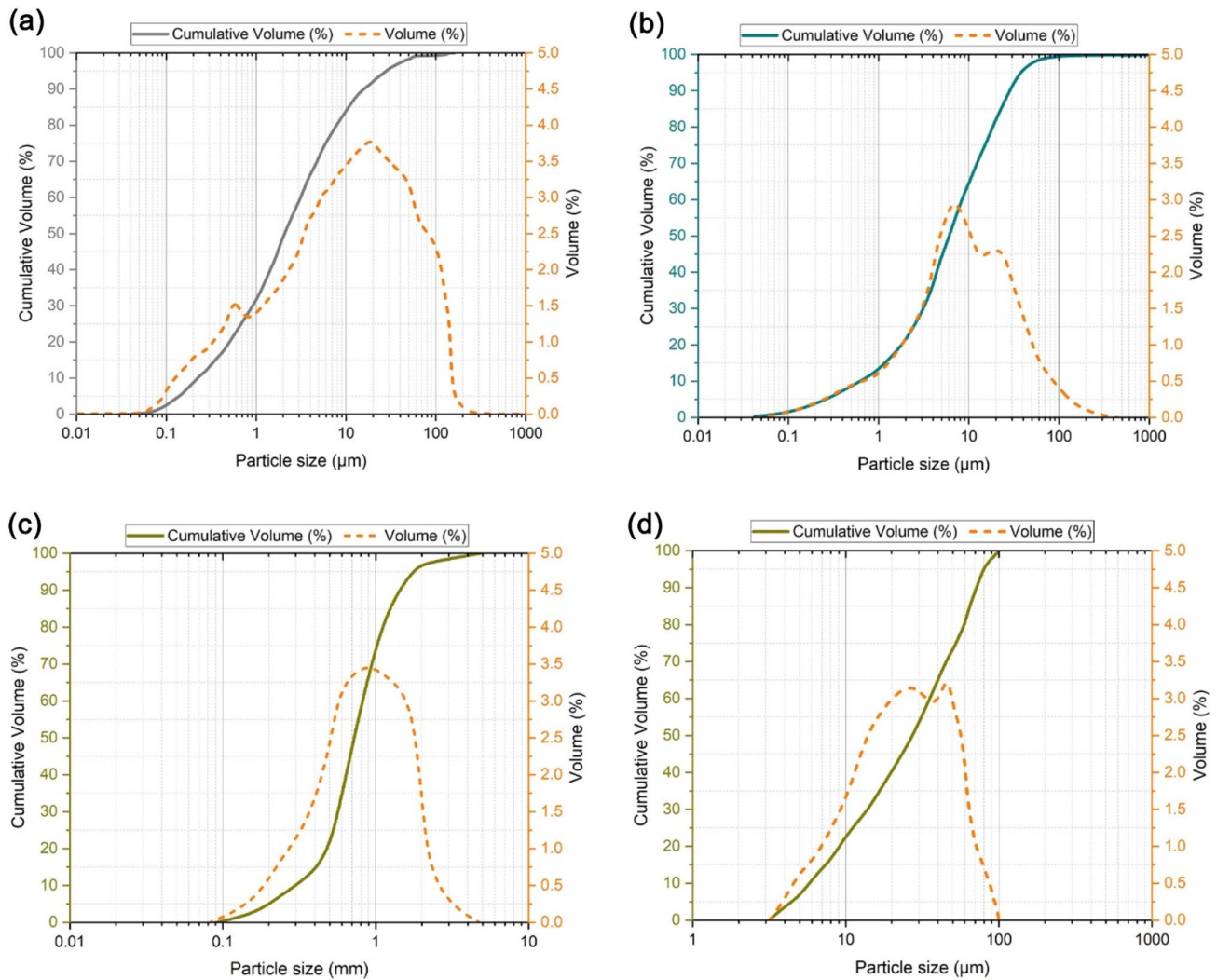
Fig. 3 Gradation analysis of materials: **a** fly ash, **b** IPMSA, **c** crusher sand, **d** lime

Table 3 Chemical composition of lime, fly ash, and IPMSA (oxides)

S. no	Oxides	Chemical composition of materials in wt%		
		Fly ash	IPMSA	Lime
1	Silica, SiO_2	41.2	8.13	0.29
2	Calcium Oxide, CaO	15.03	46.9	73.02
3	Magnesium Oxide, MgO	0.42	1.75	1.9
4	Iron Oxide, Fe_2O_3	11.54	1.5	0.34
5	Aluminum Oxide, Al_2O_3	20.85	3.72	0.64
6	Sodium Oxide, Na_2O	1.68	0.55	–
7	Potassium Oxide, K_2O	2.12	0.11	–
8	Sulfur trioxide, SO_3	1.32	0.41	–
9	Titanium dioxide, TiO_2	0.88	0.76	–
10	Phosphorus pentoxide, P_2O_5	0.67	0.32	–
11	Loss on Ignition (LOI)	4.29	35.85	23.81

in blend 1 is shown in Fig. 6a. It was noted that the brick specimens with up to 15 wt% IPMSA replacement had a compressive strength that exceeded 10 MPa, which satisfied the required strength as per BIS (IS 12894:2002). For "Class 10" bricks, the average compressive strength should not be less than 10 MPa. Also, it was noted that the increase in IPMSA content leads to a decrease in the compressive strength of bricks. Similar trends were also noted by other researchers (Singh et al. 2018). The coefficient of variation (COV) for the compressive strength of average brick specimens were found less than 6% as per BIS (IS 1077:1992). The replacement of 17.5 to 30 wt% of IPMSA gives a 32.46–69.27% strength reduction (negative impact) in bricks because IPMSA has a higher water demand due to the presence of more voids in the intermolecular structure.

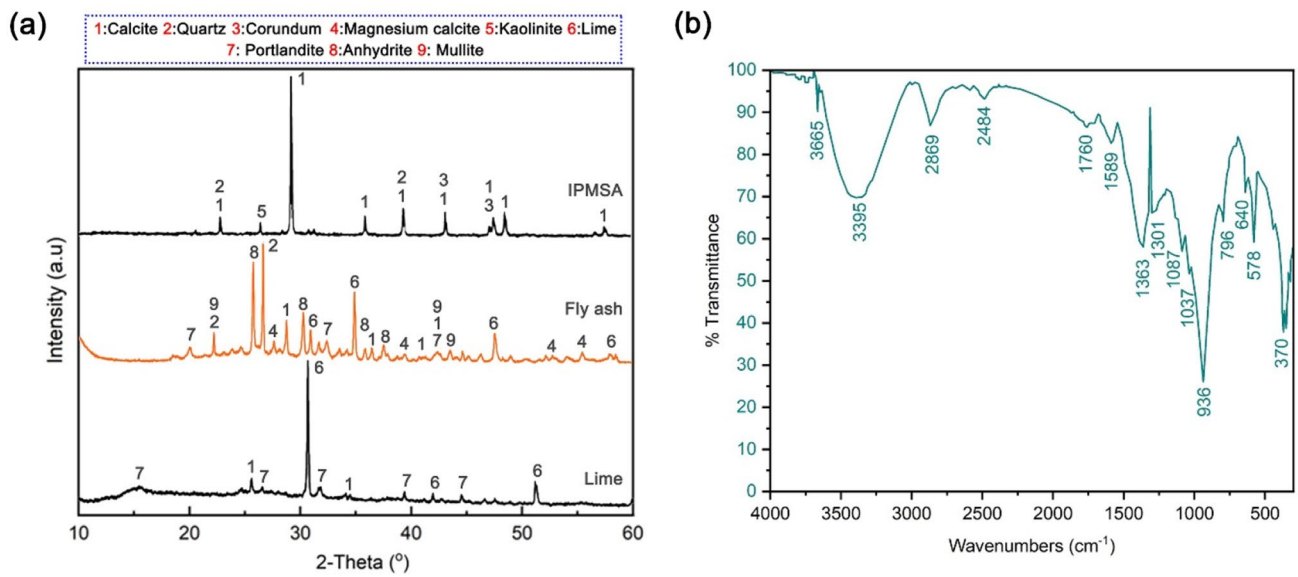Figure 6b depicts the relationship between the average compressive strength of IPMSA based FaL-G bricks

Fig. 4 **a** XRD pattern of lime, fly ash and IPMSA **b** FT-IR analysis of IPMSA

Fig. 5 SEM observations of materials: **a**, **d**, and **g** physical view of fly ash, IPMSA, and lime; **b**, **e**, and **h** Fly ash, IPMSA, and lime at 500× magnification; **c**, **f**, and **i** Fly ash, IPMSA, and lime at 2000× magnification
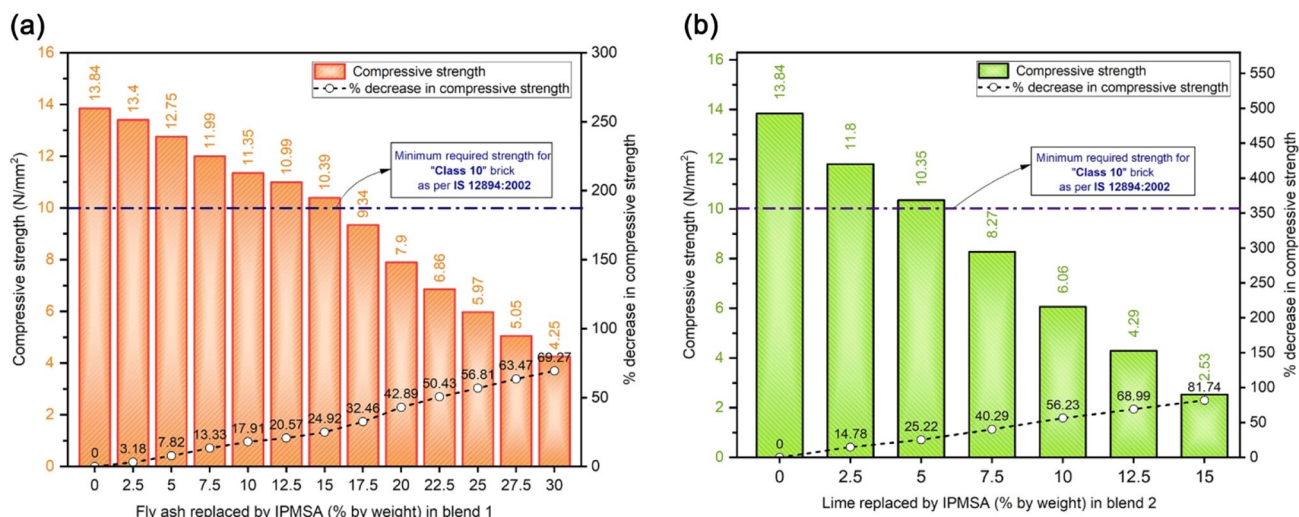
2664 B. Govindan, V. Kumarasamy
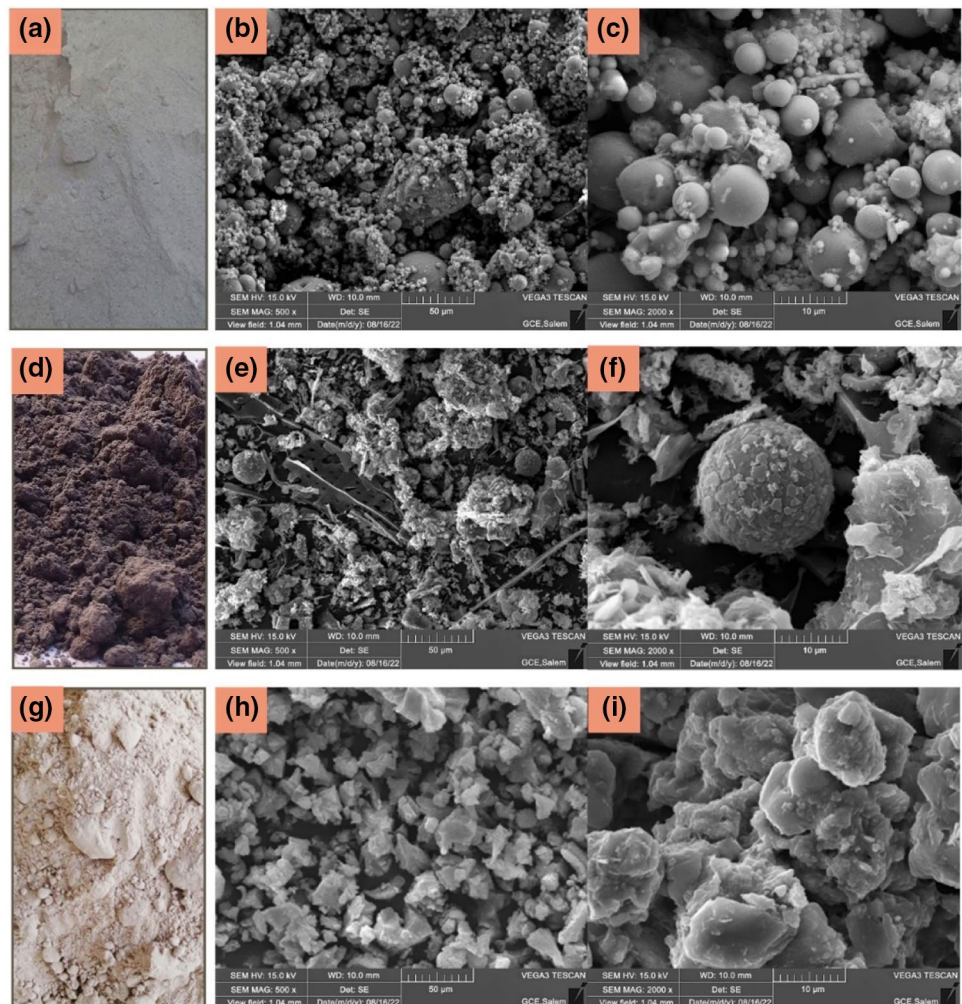
Fig. 6 Relationship between compressive strength and percentage change in compressive strength: **a** blend 1, **b** blend 2

and percentage change in compressive strength for blend 2. Similar to blend 1, IPMSA replaces lime with up to 5 wt% in blend 2, yielding satisfactory results according to BIS (IS 12894:2002), i.e., greater than 10 MPa. Also, it was observed that the increase and decrease of IPMSA and lime content leads to a drastic decrease in the compressive strength of bricks. The decrease in lime content results in the lower formation of C–S–H in bricks (Basumajumdar et al. 2005). The increase in IPMSA content leads to higher lime reactivity exhibits weak binder strength and hydration in bricks. The replacement of 7.5 to 15 wt% of IPMSA gives a 40.29–81.74% strength reduction (negative impact) in bricks.

$$\text{Fly ash} + \text{IPMSA} + \text{Lime} + \text{Gypsum} + \text{Water}$$
$$\rightarrow C-S-H + C-A-S-H + \text{Ettringite}$$

According to the compressive strength results, SEM observations have been performed for the brick mixes IPMSAB-6,14,12, and FAB-BM. Figure 7 depicts the SEM observations of the brick samples. In Fig. 7b, at 2000× magnification, more hydration products (C–A–S–H and ettringite), a strong interaction zone (a better binder matrix), and fewer voids are found in IPMSAB-6 (IPMSA replacement is 15 wt% in blend 1). The presence of the cementitious products gives the satisfactory results in accordance with Class 10 brick standards. In Fig. 7d, at 2000× magnification, hydration products are low in IPMSAB-14 (IPMSA replacement is 5 wt% in blend 2) compared to IPMSAB-6; IPMSAB-14 has fewer weak interaction zones, higher strong interaction zones (than weak interaction zones), and fewer voids and microcracks. The formations of the fewer voids and microcracks inhibit a lower compressive

strength compared to blend 1 mixes. Figure 7f shows the 2000× magnification of IPMSAB-12; from that, the number of voids and microcracks is found to be significantly higher compared to IPMSAB-6 and IPMSAB-14, resulting in a lower compressive strength and weaker binder matrix due to the presence of more voids in the microstructure, a higher water demand, and a weaker hydraulicity. Figure 7a, c, and e shows the brick SEM observations at 500× magnifications of IPMSAB-6, 14, and 12.

Dry bulk density, percentage of voids, water absorption, and efflorescence

The dry bulk density, water absorption, and percentage of voids of bricks in blends 1 and 2 are presented in Table 4. In blend 1, the IPMSA content has a greater impact on the dry bulk density than the moisture content does because IPMSA-based FaL-G bricks with a higher IPMSA content are less dense overall. The dry bulk density is inversely proportional to the increase in IPMSA content. Similar results were found in the earlier studies (Goel et al. 2021). Increases in IPMSA content up to 15 wt% can result in a decrease in dry bulk density, which may be attributable to the favorable conditions provided by high moisture content for the hydration reaction of the binder and the development of an acceptable compacted brick matrix. In addition, increasing IPMSA content might have increased water demand, which could have resulted in a decrease in dry density. The dry bulk density of all the bricks ranges from 1449.29 to 1761.89 kg/m³ in blend 1. Similar trends were observed in blend 2, replacement up to 5 wt% of IPMSA leads to acceptable compacted brick matrix.

Fig. 7 SEM observations of brick samples: **a**, **c**, and **e** IPMSAB-6, 14, and 12 at 500×magnification; **b**, **d**, and **f** IPMSAB-6, 14, and 12 at 2000×magnification
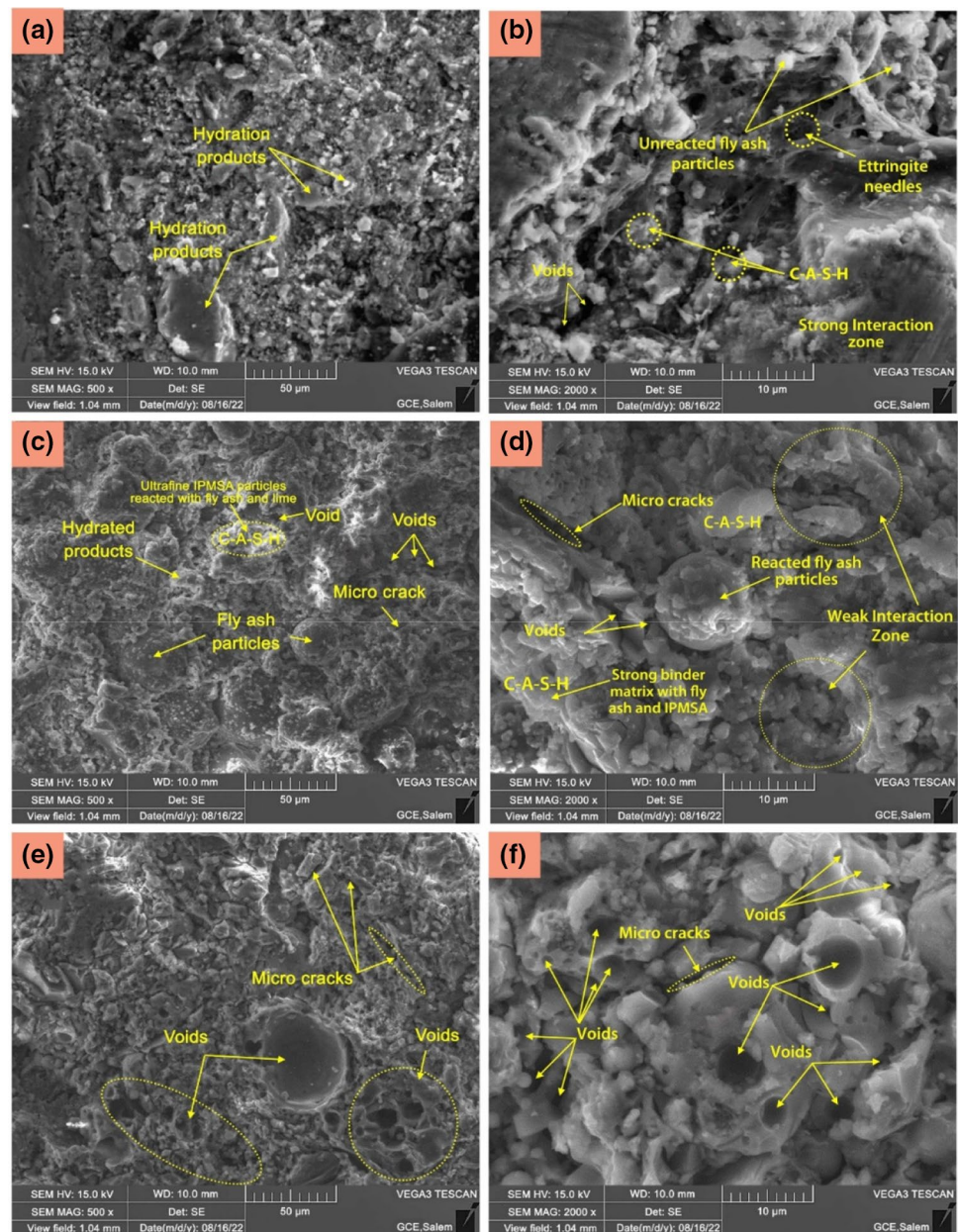
Based on Table 4, the percentage of voids increases with increase in IPMSA replacement. In blend 1, it ranges from 37.26 to 48.12% for 0 to 30 wt% of IPMSA, while in blend 2, it ranges from 40.56 to 51.94% for 0 to 15 wt% of IPMSA. In part, this increase can be attributed to the higher porosity of IPMSA. Additionally, $CaCO_3$ decomposes into calcium oxide and releases carbon dioxide, which facilitates the formation of pores to a little extent (Goel and Kalamdhad 2017). Having excessive porosity in bricks can cause them to be brittle and fragile (Dondi et al. 1997). Figure 8a–d shows the relationship between dry bulk density and water absorption, relationship between dry bulk density and percentage of voids of blends 1 and 2.

Among the parameters governing the durability of building bricks, water absorption is an important indicator of open porosity (Munir et al. 2018). Figure 9a, b shows the water absorption limits of blends 1 and 2. From the test results it was found that the water absorption values vary from 13.45–28.63% in blend 1 and 15.25–30.2% in blend 2. The replacement of IPMSA up to 17.5 wt% in blend 1 and 5 wt% in blend 2 satisfied the class 10 brick as per ASTM (ASTM C62-08:2010) and BIS (IS 12894:2002) standards (Water absorption not more than 20%). Furthermore, the dry bulk density of bricks can be inversely related to the water absorption and the percentage of voids. It can be explained by the fact that higher dry density results in a denser brick matrix and fewer voids. The replacement of IPMSA content

Table 4 Test results of dry bulk density, water absorption and percentage of voids of bricks

S. no	Mix ID	Blend	IPMSA replacement (wt%)	Dry bulk density (kg/m³)	Water absorption (%)	Percentage of voids (%)
1	FAB-BM	Blend 1 (fly ash replaced by IPMSA)	0	1761.89	12.42	36.52
2	IPMSAB-1		2.5	1690.84	13.45	37.26
3	IPMSAB-2		5	1676.63	14.41	38.74
4	IPMSAB-3		7.5	1662.42	15.73	39.38
5	IPMSAB-4		10	1648.22	16.55	40.36
6	IPMSAB-5		12.5	1636.85	17.71	41.24
7	IPMSAB-6		15	1622.64	18.74	42.36
8	IPMSAB-7		17.5	1594.22	21.39	43.14
9	IPMSAB-8		20	1574.33	23.65	44.58
10	IPMSAB-9		22.5	1540.23	24.35	45.32
11	IPMSAB-10		25	1520.34	26.36	46.10
12	IPMSAB-11		27.5	1491.92	27.62	47.28
13	IPMSAB-12		30	1449.29	28.63	48.12
14	IPMSAB-13	Blend 2 (lime replaced by IPMSA)	2.5	1676.63	15.25	40.56
15	IPMSAB-14		5	1580.01	20.86	42.38
16	IPMSAB-15		7.5	1540.23	24.72	44.68
17	IPMSAB-16		10	1491.92	26.67	46.81
18	IPMSAB-17		12.5	1443.61	28.74	49.54
19	IPMSAB-18		15	1392.46	30.20	51.94

up to 15 wt% in blend 1 and 5 wt% in blend 2 can have higher contact area, better binder matrix and formations of better hydration products according to the SEM observations. As mentioned in Sect. "Compressive strength", the higher IPMSA content (> 15 wt%) in brick mixes inhibits increased water demand and the hydration reaction, leading to a weak brick matrix. As a result of this poor brick matrix, bricks develop a high number of voids, increasing the overall void percentage and water absorption rate in blends 1 and 2.

According to BIS (IS 12894:2002) requirements for efflorescence rating (not more than moderate), "slight" efflorescence was found in brick specimens having higher IPMSA content (blends 1 and 2) after the exposure period. The surface of the specimens did not show any flaking or cracking.

Dynamic modulus of elasticity

Figure 10a, b depicts the dynamic modulus of elasticity (E_d) for blends 1 and 2. With an increase in IPMSA content of 15 wt% in blend 1 and 2.5 wt% in blend 2, almost very few changes is observed in the dynamic modulus of elasticity. Bricks containing more than 15 wt% IPMSA in blend 1 had a lower dynamic modulus of elasticity value. Similar trends were found for the blend 2 bricks where the IPMSA content increases. When the brick matrix contains more voids in higher IPMSA content, the ultrasonic pulse velocity is reduced, which lowers the dynamic modulus of elasticity. The lower UPV values of bricks owing to the heterogeneity

of unevenly distributed grains and incomplete hydration reactions lead to low dynamic modulus of elasticity in blends 1 and 2. The replacement of IPMSA up to 15 wt% in blend 1 and 5 wt% in blend 2 can provide a homogenous distribution of particles in the brick matrix; it can be concluded from the results.

Impact strength

Table 5 shows the impact energy value of various bricks in blends 1 and 2. The impact loading before and after for the one set of brick samples is shown in Fig. 11a, b. Consistently, the brick's transition zone showed the first crack. It is likely that cracks will move toward the center of the specimen as the number of drops increases. It has been observed that cracks may be caused by both transient regions in some cases. Javan et al. observed similar crack failure patterns when impact loading interlocking bricks (Rezaee Javan et al. 2017).

From Table 5, the fly ash is replaced by IPMSA having higher N_f values as well as higher impact energy. Impact energy resistance is highly related to the hydration products, contact area and brick binder matrix of the bricks. Contact area between hydration products and particles is a key factor in preventing crack propagation under impact energy (Siddique et al. 2018). In previous sections, hydration products and IPMSA particles can have better contact areas, which results in a better binder matrix at lower densities. At the
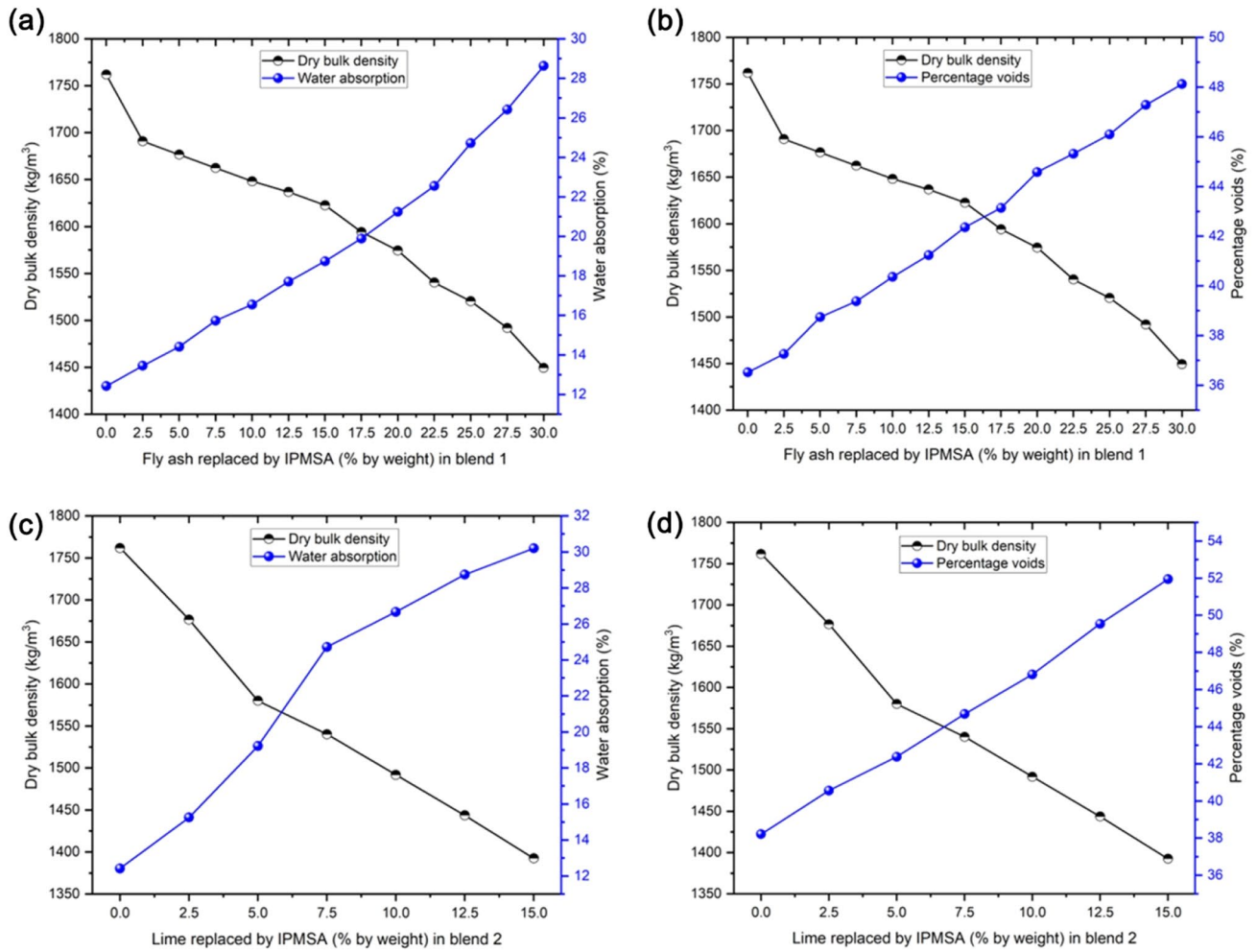
Fig. 8 Relationship between dry bulk density and water absorption: **a** blend 1 and **c** blend 2; Relationship between dry bulk density and percentage of voids: **b** blend 1 and **d** blend 2
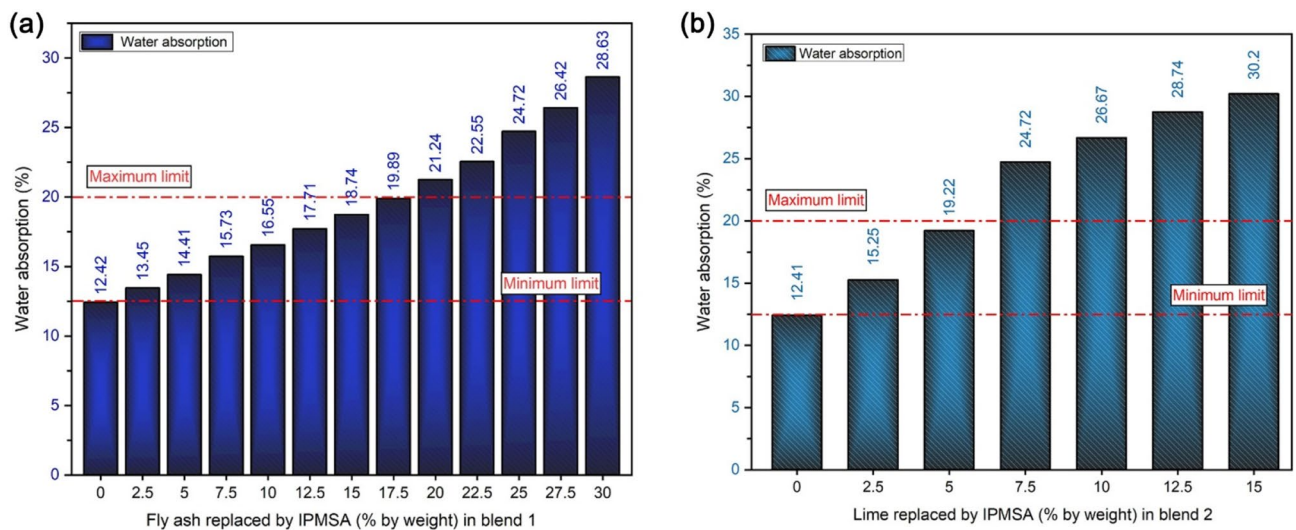

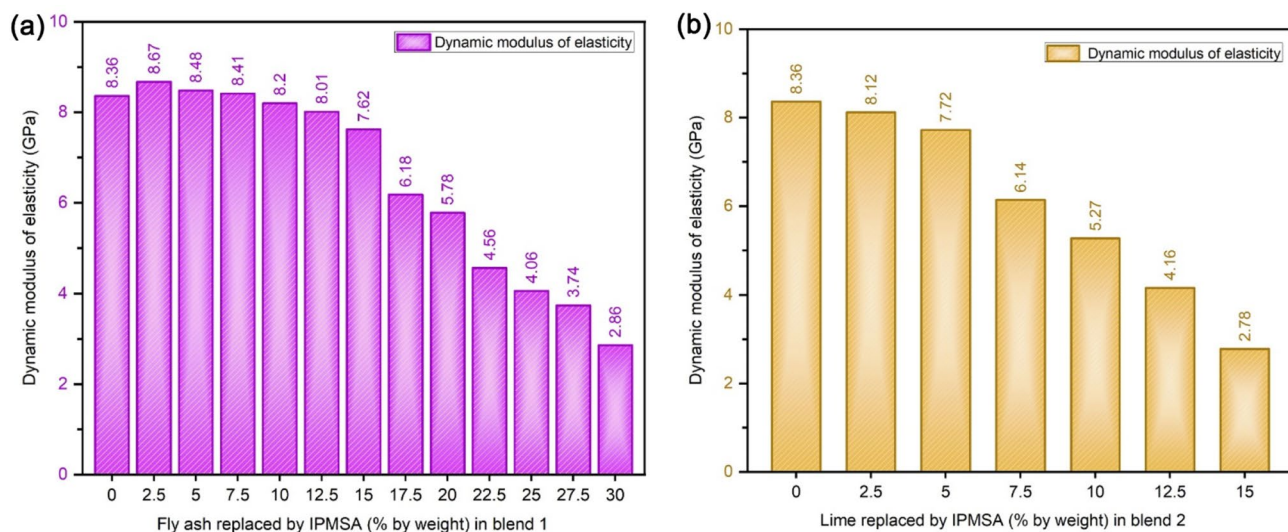**Fig. 9** Water absorption of bricks: **a** blend 1 and **b** blend 2

Fig. 10 Dynamic modulus of elasticity: **a** blend 1 and **b** blend 2

Table 5 Test results of impact energy of bricks

S. no	Mix ID	Blend	IPMSA replacement (wt%)	N_i	N_f	Impact energy (I_e)
1	FAB-BM	Blend 1 (Fly ash replaced by IPMSA)	0	32.667	44.333	320.46
2	IPMSAB-1		2.5	32.000	39.667	313.92
3	IPMSAB-2		5	30.333	38.667	297.57
4	IPMSAB-3		7.5	29.667	36.333	291.03
5	IPMSAB-4		10	28.333	33.667	277.95
6	IPMSAB-5		12.5	27.667	32.333	271.41
7	IPMSAB-6		15	27.333	31.667	268.14
8	IPMSAB-7		17.5	26.333	28.333	258.33
9	IPMSAB-8		20	25.667	27.333	251.79
10	IPMSAB-9		22.5	25.000	26.333	245.25
11	IPMSAB-10		25	23.667	25.667	232.17
12	IPMSAB-11		27.5	23.333	24.333	228.90
13	IPMSAB-12		30	22.333	23.667	219.09
14	IPMSAB-13	Blend 2 (Lime replaced by IPMSA)	2.5	30.667	40.667	300.84
15	IPMSAB-14		5	27.333	33.667	268.14
16	IPMSAB-15		7.5	25.667	30.667	251.79
17	IPMSAB-16		10	22.333	25.667	219.09
18	IPMSAB-17		12.5	20.000	20.333	196.20
19	IPMSAB-18		15	18.333	18.667	179.85

same time, the higher replacement of IPMSA (> 15 wt% in blend 1 and > 5 wt% in blend 2) in blends 1 and 2 got very lower impact energy in accordance with lower N_f values observed. Specifically, particles with IPMSA have better hydration product due to their fineness, which resulted in an improved contact area between the hydration product and particles. Similarly, bricks in blend 1 (up to replacement 15 wt% of IPMSA) with a higher concentration of hydration products may make bricks harder to resist the impacts. In

addition to blend 1, bricks have an average increase of 12% impact energy than blend 2 bricks.

Drying shrinkage

Table 6 shows the drying shrinkage value for IPMSA-based FaL-G bricks in blends 1 and 2. For all brick mixes, drying shrinkage does not exceed 0.15% as stipulated in BIS (IS 12894:2002). The blend 1 mix showed the lowest drying
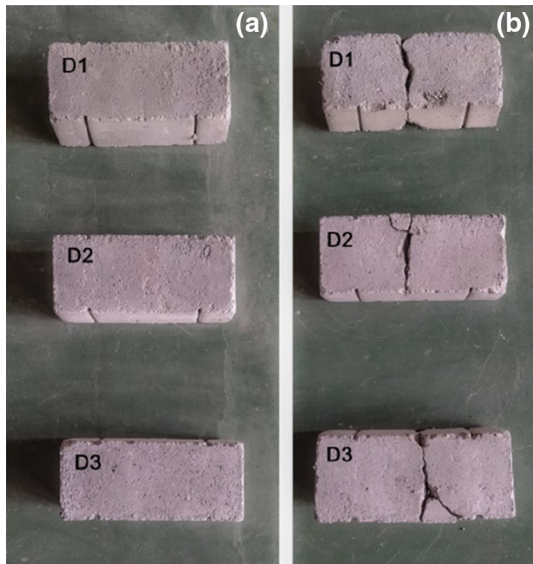
Fig. 11 Typical failure pattern observed on the samples of one set of IPMSA based FaL-G bricks: **a** before impact load, **b** after impact load

shrinkage (5 wt% IPMSA), while the blend 2 mix showed the highest drying shrinkage (15 wt% IPMSA).

It is evident from the drying shrinkage results (Table 6) that the higher content of IPMSA significantly affects the drying shrinkage of the bricks. As discussed, drying shrinkage can also be defined as the difference in length between the saturated and dry states of bricks during drying. As more water was lost during drying, shrinkage increased, which was correlated with greater water absorption at corresponding mixes. However, it was determined that this increase of IPMSA content (> 15 wt% in blend 1 and > 5 wt% in blend 2) was not significant. Other researchers are also found similar results when free water is removed from ceramic materials(Searle and Grimshaw 1959). IPMSA (> 5 wt%) content may have played a role in the inconsistent shrinkage trend observed in blend 2 due to the change in dominant factor.

Thermal conductivity

Heat transfer through masonry units is heavily influenced by the thermal conductivity of the materials. Measurements can be taken at two extremes, namely in completely dry and saturated conditions. As is well known, thermal conductivity is greater under saturated conditions than under dry conditions. In another aspect, the thermal conductivity of the bricks is directly proportional to the percentage of voids present in the bricks. Based on the results shown in Table 6, similar results were obtained for FaL-G bricks incorporated with IPMSA. The lower thermal conductivity is observed in the FAB-BM mix (IPMSA is 0 wt%), and the higher thermal conductivity

is found in the IPMSAB-18 mix (IPMSA is 15 wt%) in blend 2. As discussed earlier in Sect. "Dry bulk density, percentage of voids, water absorption, and efflorescence", the higher replacement of IPMSA content generates a higher percentage of voids in blends 1 and 2 due to their higher surface areas and having more voids in the microstructure. Specifically, in complete saturation conditions, the IPMSA based FaL-G bricks can have higher water absorption, and the heat conduction is very high. Similar to that, in completely dry conditions, the heat conduction of the bricks was low. So, the thermal conductivity of the bricks was found to be slightly similar to the mixes up to 15 wt% of IPMSA in blend 1 and 5 wt% of IPMSA in blend 2. Other researchers have found similar results with FaL-G bricks (Goel et al. 2021). Figure 12a, b depicts the relationship between the percentage of voids and thermal conductivity of the bricks under complete dry and saturated conditions for blends 1 and 2.

Chemical characterization

Construction materials like sand/lime or silica/lime bricks are produced primarily through the formation of $CaO–SiO_2–H_2O$ (C–S–H) (Basumajumdar et al. 2005). As a result of C–S–H phase formation, fly ash bricks were able to adhere to it. Also, hydrogarnet forms as $CaO–Al_2O_3–SiO_2–H_2O$ (C–A–S–H) with Al_2O_3 (Goñi et al. 2003). C–S–H and C–A–S–H phases are primarily responsible for hardening fly ash/lime bricks due to their high Al_2O_3 and SiO_2 contents.

Following is an explanation of the chemical reaction system for the bricks. In the beginning, the CaO, SiO_2, and Al_2O_3 in the brick interact with one another to produce pozzolanic active minerals such as belite (Ca_2SiO_4) and gehlenite ($Ca_2Al[AlSiO_7]$). While gehlenite is directly hydrated with water, $Ca(OH)_2$ and C–S–H gel are also produced (Zhang et al. 2019). These compounds increase brick strength. Similar to that, gehlenite reacts with $Ca(OH)_2$ to produce C–A–S–H gels (Y Xu et al. 2014).

According to Sect. "Compressive strength" the XRD pattern are examined. Figure 13 depicts the XRD patterns of the FAB-BM and FaL-G bricks incorporated with IPMSA. The major crystalline phases of the control brick specimen are quartz (SiO_2), mullite ($3Al_2O_3 \cdot 2SiO_2$), and calcite ($CaCO_3$). It also contains belite (Ca_2SiO_4) and gehlenite ($Ca_2Al[AlSiO_7]$) as minor components. The XRD pattern of bricks with IPMSA incorporation contains the same major crystalline phases as the previous pattern, including quartz (SiO_2), mullite ($3Al_2O_3 2SiO_2$), and calcite ($CaCO_3$). It is not observed that IPMSA leads to any phase transformations and increases porosity. Other researchers also found similar results (Singh et al. 2018).

Table 6 Test results of drying shrinkage and thermal conductivity of bricks

S. no	Mix ID	Blend	IPMSA replacement (wt%)	Drying shrinkage (10^{-3}) %	Thermal conductivity (W/m K)	
					Dry condition	Saturated condition
1	FAB-BM	Blend 1 (fly ash replaced by IPMSA)	0	24.86	0.342	1.668
2	IPMSAB-1		2.5	21.24	0.349	1.702
3	IPMSAB-2		5	23.78	0.363	1.769
4	IPMSAB-3		7.5	26.84	0.369	1.799
5	IPMSAB-4		10	29.67	0.378	1.843
6	IPMSAB-5		12.5	34.22	0.386	1.884
7	IPMSAB-6		15	37.89	0.397	1.935
8	IPMSAB-7		17.5	58.14	0.404	1.970
9	IPMSAB-8		20	65.67	0.417	2.036
10	IPMSAB-9		22.5	81.29	0.424	2.070
11	IPMSAB-10		25	94.26	0.432	2.106
12	IPMSAB-11		27.5	103.44	0.443	2.159
13	IPMSAB-12		30	124.56	0.451	2.198
14	IPMSAB-13	Blend 2 (lime replaced by IPMSA)	2.5	23.46	0.364	1.724
15	IPMSAB-14		5	38.29	0.380	1.801
16	IPMSAB-15		7.5	59.82	0.401	1.899
17	IPMSAB-16		10	76.98	0.420	1.990
18	IPMSAB-17		12.5	113.25	0.445	2.106
19	IPMSAB-18		15	138.15	0.466	2.208
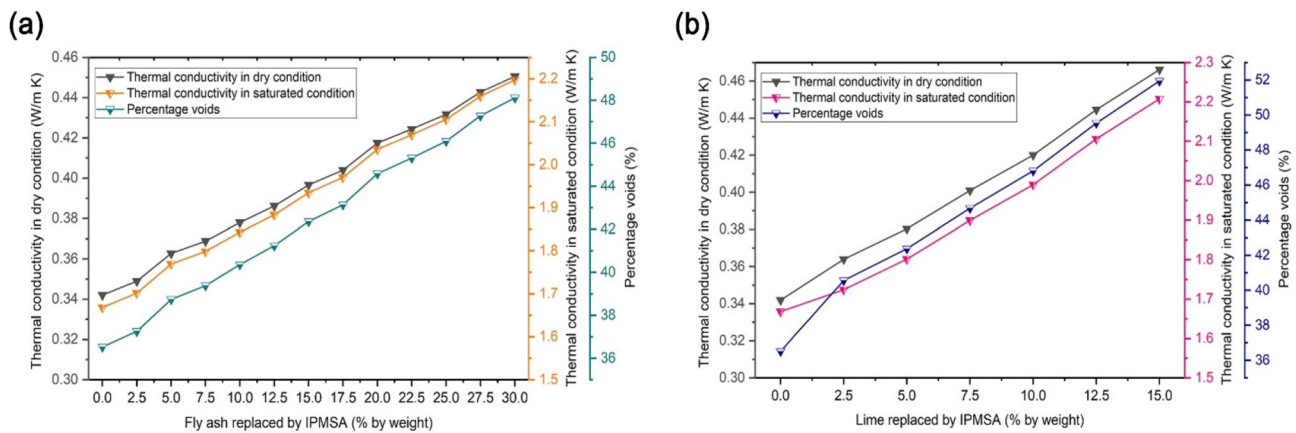
Fig. 12 Thermal conductivity of IPMSA based FaL-G bricks in complete dry and saturated conditions: **a** blend 1, **b** blend 2

Analysis of FaL-G bricks incorporated with IPMSA: A Comparison with clay brick and fly ash brick

The suitability of the developed bricks is compared in Table 7 with fly ash bricks as per BIS (IS 12894:2002) and burnt clay bricks as per BIS (IS 1077:1992) standards. From the test results, bricks with replacement up to 15 wt% in blend 1 (fly ash replaced by IPMSA) and replacement up to 5 wt% in blend 2 (lime replaced by IPMSA) satisfy the requirements of "class 10" bricks as per BIS (IS 1077:1992;

IS 12894:2002) standards. Water absorption rates in the optimized bricks are less than the permissible limit (< 20%). The drying shrinkage test results revealed that the optimized bricks in blends 1 and 2 had similar properties. The drying shrinkage for the optimized bricks is also found to be within the permissible limit (< 0.15%). The thermal conductivity of the conventional clay brick is 0.551 W/m K (Singh et al. 2018). The maximum thermal conductivity for the optimized bricks is 0.397 W/m K and 0.380 W/m K. It reveals that the developed bricks' thermal insulation was better than
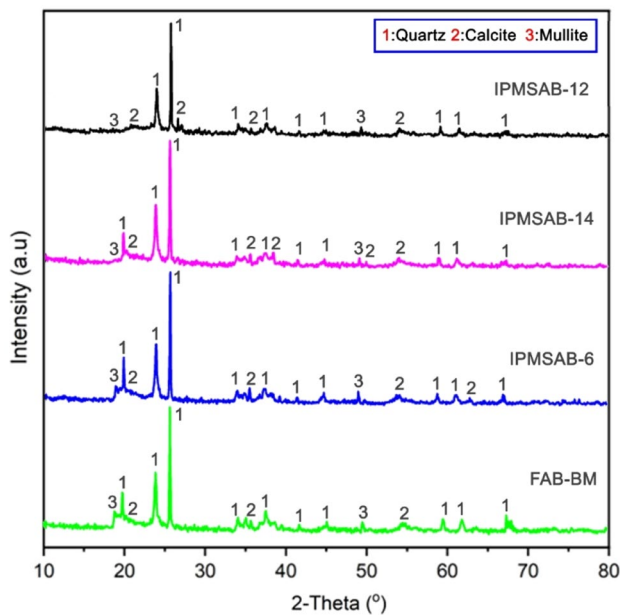
Fig. 13 XRD patterns of IPMSA-based FaL-G bricks

conventional burnt clay bricks and slightly similar to the base mix.

Conclusion

Incinerated paper mill sludge ash (IPMSA) can be sustainably utilized in manufacturing building bricks as a partial replacement for fly ash and lime. Following the above experimental results and discussion on the developed bricks, the following conclusions are drawn:

- The replacement of IPMSA in the FaL-G mix resulted in decreased compressive strength. The maximum amount of IPMSA addition in the mix, which satisfied the minimum compressive strength requirement of various building standards, including "class 10" of BIS (IS 12894:2002), was 15 wt% in blend 1 and 5 wt% in blend 2.

- Brick durability is directly related to water absorption. Higher addition of IPMSA leads to higher water absorption, higher percentage of voids, lower bulk densities, and higher thermal conductivity. As a result of a higher IPMSA addition, the specimens had an asymmetrical, interconnected porous structure. However, IPMSA up to 15 wt% in blend 1 and 5 wt% in blend 2 provides satisfactory requirements with BIS (IS 12894:2002) standards.

- The addition of IPMSA to fly ash bricks exceeds 15 wt% in blend 1 and 5 wt% in blend 2. These bricks do not conform to the standards for fly ash bricks due to their high-water absorption and low compressive strength.

- The drying shrinkage of all the developed bricks is within the permissible limit (< 0.15%).

- XRD patterns reveal that adding IPMSA leads to any phase transformations and increases porosity. SEM observations revealed that the replacement of IPMSA up to 15 and 5 wt% in blends 1 and 2 provided the formation of higher hydration products that resulted in a better binder matrix in the form of stronger and fewer weaker interaction zones and a lower porosity to satisfy the strength requirements as per the standards. In addition, blend 1 bricks have an average increase in impact energy of 12% over blend 2 bricks.

- The brick matrix contains more voids in higher IPMSA content; the ultrasonic pulse velocity is reduced, which lowers the dynamic modulus of elasticity. Optimized brick mixes' dynamic modulus of elasticity is slightly similar to the base mix.

- For the first time, this study provided a new method of producing FaL-G bricks by sustainably incorporating IPMSA and reducing the fly ash and lime content up to 15 and 5 wt%, thereby reducing the fly ash and lime demand.

- Furthermore, the work has been extended to better understand the exact mechanism of bricks by analyzing the microstructure and durability properties in detail.

The production of Fal-G bricks incorporated with IPMSA has a more positive impact in terms of advanced waste management, environmental protection, and reducing lime and

Table 7 Properties of standard and developed bricks: a comparison

S. no	Properties	Clay brick	Fly ash brick	Developed bricks	
		IS 1077:1992 (Class 10)	IS 2894:2002 (Class 10)	IS 12894:2002	
				IPMSAB-6	IPMSAB-14
1	Compressive strength (N/mm^2)	≥ 10	≥ 10	10.39	10.35
2	Water absorption	< 20%	< 20%	18.74	19.22
3	Efflorescence	Moderate	Slight to moderate	Nil	Nil
4	Drying shrinkage (%)	–	< 0.15%	0.037%	0.038%
5	Thermal conductivity (W/m K)	–	–	0.397	0.380

fly ash consumption. A further advantage is that the land requirement for producing IPMSA-based FaL-G bricks is less than for burnt clay bricks. In addition to reducing land requirements, establishing near-demand areas/habitations helps reduce transport costs due to the reduced land requirement and environmentally friendly production. The method reduces the chance of breakage and reduces transportation costs. Using industrial by-products to manufacture bricks can significantly reduce the amount of waste discharged to landfills or ash dumps to create a sustainable solution.

Declarations

Conflict of interest The authors declare no conflict of interest.

Ethical approval This article does not contain any studies with human participants or animals performed by any authors.

References

ASTM C618:2012 Standard specification for coal fly ash and raw or calcined natural pozzolan for use in concrete

ASTM C62–08:2010 Standard specification for building brick (solid masonry units made from clay or shale). American Society for Testing and Materials, USA

ASTM C642:2021 Standard test method for density, absorption, and voids in hardened concrete, 2021st edn. American Society for Testing and Materials, USA

Balaguera A, Carvajal GI, Albertí J, Fullana-i-Palmer P (2018) Life cycle assessment of road construction alternative materials: a literature review. Resour Conserv Recycl 132:37–48. https://doi.org/10.1016/j.resconrec.2018.01.003

Basumajumdar A, Das AK, Bandyopadhyay N, Maitra S (2005) Some studies on the reaction between fly ash and lime. Bull Mater Sci 28:131–136. https://doi.org/10.1007/BF02704232

Chin WQ, Lee YH, Amran M et al (2022) A sustainable reuse of agro-industrial wastes into green cement bricks. Materials 15:1713. https://doi.org/10.3390/ma15051713

Cicek T, Tanrıverdi M (2007) Lime based steam autoclaved fly ash bricks. Constr Build Mater 21:1295–1300. https://doi.org/10.1016/j.conbuildmat.2006.01.005

Coates J (2006) Interpretation of infrared spectra, a practical approach. In: Meyers RA (ed) Encyclopedia of analytical chemistry. Wiley, Chichester, UK

CSE analysis (2021) CSE analysis; data sourced from CEA's annual ash reports 2010-11 to 2020-21

Deviatkin I, Kujala A, Horttanainen M (2015) Deinking sludge utilization possibilities: technical, economic, and environmental assessments. LUT-Univ 4:112–120

Dondi M, Marsigli M, Fabbri B (1997) Recycling of industrial and urban wastes in brick production: a review. Tile Brick Int 13:218–225

Frías M, Rodríguez O, Sánchez de Rojas MI (2015) Paper sludge, an environmentally sound alternative source of MK-based cementitious materials. Rev Constr Build Mater 74:37–48. https://doi.org/10.1016/j.conbuildmat.2014.10.007

Furlani E, Brückner S, Minichelli D, Maschio S (2008) Synthesis and characterization of ceramics from coal fly ash and incinerated paper mill sludge. Ceram Int 34:2137–2142. https://doi.org/10.1016/j.ceramint.2007.08.002

Gencel O, Koksal F, Ozel C, Brostow W (2012) Combined effects of fly ash and waste ferrochromium on properties of concrete. Constr Build Mater 29:633–640. https://doi.org/10.1016/j.conbuildmat.2011.11.026

Goel G, Kalamdhad AS (2017) An investigation on use of paper mill sludge in brick manufacturing. Constr Build Mater 148:334–343. https://doi.org/10.1016/j.conbuildmat.2017.05.087

Goel G, Vasić MV, Katiyar NK et al (2021) Potential pathway for recycling of the paper mill sludge compost for brick making. Constr Build Mater 278:122384. https://doi.org/10.1016/j.conbuildmat.2021.122384

Goñi S, Guerrero A, Luxán MP, Macías A (2003) Activation of the fly ash pozzolanic reaction by hydrothermal conditions. Cem Concr Res 33:1399–1405. https://doi.org/10.1016/S0008-8846(03)00085-1

Grau F, Choo H, Hu J, Jung J (2015) Engineering behavior and characteristics of wood ash and sugarcane bagasse ash. Materials 8:6962–6977. https://doi.org/10.3390/ma8105353

Gupta T, Chaudhary S, Sharma RK (2016) Mechanical and durability properties of waste rubber fiber concrete with and without silica fume. J Clean Prod 112:702–711. https://doi.org/10.1016/j.jclepro.2015.07.081

Indian paper industry: out of the woods (2016) CARE rating on Credit Perspective: Paper Industry, http://www.careratings.com

IS 1077:1992 Common burnt clay building bricks specifications. Bureau of Indian Standards, New Delhi, India.

IS 12894:2002 Pulverized fuel ash-lime bricks. Bureau of Indian Standards, New Delhi

IS 13311 (Part 1):1992 Non-destructive testing of concrete - methods of test. Bureau of Indian Standards, New Delhi, India

IS 2720 (part II): 1973 Methods of test for soils part II determination of water content. Bureau of Indian Standards, New Delhi, India.

IS 3495 (Parts 1 to 4):1992 Methods of tests of burnt clay building bricks. Bureau of Indian Standards, New Delhi

IS 3812 (Part-1):2003 Specification for pulverized fuelash. Bureau of Indian Standards, New Delhi

IS 383:2016 Coarse and fine aggregate for concrete-specification. Bureau of Indian Standards, New Delhi, India

IS 4139:1989 Calcium silicate bricks. Bureau of Indian Standards, New Delhi, India.

IS 456:2000 Indian standard plain and reinforced concrete code of practice. Bureau of Indian Standards, New Delhi

IS 712:1984 Specification for building limes. Bureau of Indian Standards, New Delhi, India

Lind EE, Grahn M (2011) Directional genetic selection by pulp mill effluent on multiple natural populations of three-spined stickleback (Gasterosteus aculeatus). Ecotoxicology 20:503–512. https://doi.org/10.1007/s10646-011-0639-8

Munir MJ, Kazmi SMS, Wu Y-F et al (2018) Thermally efficient fired clay bricks incorporating waste marble sludge: an industrial-scale study. J Clean Prod 174:1122–1135. https://doi.org/10.1016/j.jclepro.2017.11.060

Raut SP, Sedmake R, Dhunde S et al (2012) Reuse of recycle paper mill waste in energy absorbing light weight bricks. Constr Build Mater 27:247–251. https://doi.org/10.1016/j.conbuildmat.2011.07.053

Rezaee Javan A, Seifi H, Xu S et al (2017) The impact behaviour of plate-like assemblies made of new interlocking bricks: an experimental study. Mater Des 134:361–373. https://doi.org/10.1016/j.matdes.2017.08.056

Saxena R, Siddique S, Gupta T et al (2018) Impact resistance and energy absorption capacity of concrete containing plastic waste. Constr Build Mater 176:415–421. https://doi.org/10.1016/j.conbuildmat.2018.05.019

Searle AB, Grimshaw RW (1959) The chemistry and physics of clays and other ceramic materials

Shivasakthivadivelan RA (2022) (2022) Study on the properties of innovative green brick subjected to varying temperature and time. Int J Coal Prep Util. https://doi.org/10.1080/19392699.2022.2064456

Siddique S, Shrivastava S, Chaudhary S, Gupta T (2018) Strength and impact resistance properties of concrete containing fine bone china ceramic aggregate. Constr Build Mater 169:289–298. https://doi.org/10.1016/j.conbuildmat.2018.02.213

Singh SK, Kulkarni S, Kumar V, Vashistha P (2018) Sustainable utilization of deinking paper mill sludge for the manufacture of building bricks. J Clean Prod 204:321–333. https://doi.org/10.1016/j.jclepro.2018.09.028

Sutcu M, del Coz Díaz JJ, Álvarez Rabanal FP et al (2014) Thermal performance optimization of hollow clay bricks made up of paper waste. Energy Build 75:96–108. https://doi.org/10.1016/j.enbuild.2014.02.006

Xu Y, Li JX, Kan LL (2014) Study on composite cementitious material prepared by calcinating phosphogypsum. Bull Chin Ceram Soc 33:953–958

Zhang WS, Zhang JT, Ye JY et al (2019) Structure and activity of dicalcium silicate. J Chin Ceram Soc 368:146–152

Zmamou H, Leblanc N, Levacher D, Kubiak J (2021) Recycling of high quantities of wastepaper sludge ash for production of blended cements and alternative materials. Environ Technol Innov 23:101524. https://doi.org/10.1016/j.eti.2021.101524